



Doping of boron in TiO₂ catalyst: Enhanced photocatalytic degradation of antibiotic under visible light irradiation

Esra Bilgin Şimşek*

Yalova University, Chemical and Process Engineering Department, 77100, Yalova, Turkey

ARTICLE INFO

Article history:

Received 16 June 2016

Received in revised form 07 October 2016

Accepted 07 October 2016

Available online 16 March 2017

Research Article

Keywords:

Antibiotics degradation,

Boron doped TiO₂,

Photocatalysis

Visible light

ABSTRACT

A series of B-doped anatase TiO₂ catalysts have been synthesized by solvothermal method and the photocatalytic activity toward a fluoroquinolone antibiotic (ciprofloxacin) has been investigated. The results showed that the boron doping not only reduced the band gap energy, it also improved the photocatalytic activity of TiO₂ towards the selected antibiotic under visible light irradiation. The effects of solution pH, catalyst dosage and the presence of process enhancer/inhibitors on the photoactivity were examined. Response surface methodology was successfully utilized to model and optimize the photocatalytic process with high correlation ($R^2 = 0.9960$). The degrees of boron doping and visible light active mechanism have also been studied. Compared with raw TiO₂ boron doped catalysts exhibit excellent photostability and photodegradation ability of ciprofloxacin under visible light irradiation.

1. Introduction

Antibiotics are one of the most used pharmaceutical groups in human and veterinary medicine. Although they are metabolized within the body, approximately 90% of orally administered doses are excreted unmetabolized and frequently monitored at sub-inhibitory concentrations in sediments as well as surface water, groundwater, and drinking water [1, 2]. Ciprofloxacin (1-cyclopropyl-6-fluoro-4-oxo-7-(piperazin-1-yl)-quinoline-3-carboxylic-acid), is a fluoroquinolone antibiotic and an antibacterial agent globally used for curing bacterial infections in humans and animals [3]. Ciprofloxacin (CIP) is very persistent in aquatic environments [2] and has been detected in different water systems [4]. It has also been found in the effluent streams of drug production facilities (up to 31 mg/L) [5] and hospitals (up to 150 µg/L) [6]. It can also accumulate in the ground when ciprofloxacin-polluted sludge is applied as fertilizer [6].

As the common processes such as sewage treatment, biodegradation, sorption and hydrolysis are insufficient for the treatment of antibiotics [7]; photocatalytic technology is very effective advanced oxidation process for the removal of antibiotics in the environment [8–12]. Titanium dioxide (TiO₂) is a dominant photocatalyst owing to its robust oxidizing power, photochemical corrosive resistance and nontoxicity [2, 13]. However, TiO₂ has some disadvantages like due to its

wide band gap it can be only induced by the UV light which limits its suitable application in the wastewater treatment [13, 14]. Doping of metal or non-metal ions is one of the promising method to enhance the visible light absorption and increase the photoactivity via forming impurity levels in the forbidden band [15–18]. Boron as a dopant has recently drawn attention as the photocatalytic performance increased significantly when compared with raw TiO₂ [18–24]. The incorporation of boron into TiO₂ catalyst can extend the absorption band-edge to the visible region [22–29]. Zhao et al. [26] proposed that the boron was incorporated into TiO₂ catalyst rather than existing in a separate phase (B₂O₃ or H₃BO₃) and occurs as the chemical states of B-Ti-B/B-O or B-Ti-O). Štengl et al. [27] reported that boron (III) oxide doped TiO₂ presented higher photocatalytic degradation rate for Orange II dye in comparison with the raw TiO₂ sample under visible-light irradiation. Uddin et al. [28] synthesized B/N/Ag co-doped carbon nanotube (CNT)-TiO₂ thin films and found that methylene blue degradation was significantly increased when after co-doping. Zaleska et al. [22] prepared B-TiO₂ catalysts by surface impregnation procedure and found that the degradation of phenol were strongly influenced depended on the synthesis manner of boron doped TiO₂ catalysts.

To the best of our knowledge and on the basis of the literature search, the photocatalytic degradation of

*Corresponding author: ebilgin.simsek@yalova.edu.tr

ciprofloxacin over B doped TiO₂ catalysts under UV-A and visible-light irradiation has been investigated for the first time in this study. The effects of boron content, initial pH, catalyst dosage and the presence of process enhancers/inhibitors on the photocatalytic process were investigated.

2. Materials and methods

2.1. Chemicals and reagents

All chemicals were obtained commercially and used without further purification. Ciprofloxacin (98%) was obtained from Acros Organics.

2.2. Synthesis of B-doped TiO₂ catalysts

Boron doped TiO₂ catalysts were prepared by a modified solvo-thermal procedure previously reported [19]. The desired amount of boric acid were dissolved in ethanol, then PEG-600 was added adjusting the pH with concentrated nitric acid. Then, tetrabutyl titanate in ethanol was dripped into the boric acid solution under magnetic stirring. After aging time, the gel was operated by hydrothermal treatment in a Teflon-lined stainless steel autoclave at 180 °C for 10 h. After calcination at 500 °C, the powder was ground up after cooling to room temperature. B-doped TiO₂ catalysts were prepared with weight content of boron: 2.0, 4.0, 6.0 and 8.0 wt.%. The blank sample of TiO₂ was prepared by the similar reaction above (without addition of H₃BO₃).

2.3. Characterization studies

The UV-visible diffusion reflectance spectra (UV-vis DRS) of catalysts recorded with spectrophotometer (Perkin Elmer Lambda 35) using BaSO₄ as the reference standard. The morphology of catalysts was investigated by using scanning electron microscope (SEM) equipped with a Bruker energy dispersive X-Ray (EDX) detector (Philips XL30 ESEM-FEG/EDAX).

2.4. Photocatalytic degradation experiments

Photocatalytic degradation studies were performed in a laboratory scale column-shaped stainless steel cabinet equipped with a hexagonally placed 18 UV-A lamps (Philips TL 8W Actinic BL, mainly emits 365 nm). Visible light irradiation tests were conducted in a square photo-reactor donated with visible metal halide lamps (Osram 150 W, λ:400–800 nm). For each deg-

radation experiment, CIP concentrations of 20 mg L⁻¹ were prepared in 50 mL double distilled water followed by adjusting the pH. Before the photocatalytic experiments, the solution was stirred for 30 min in dark to achieve adsorption equilibrium. Aliquots of the suspension (5 mL) were periodically collected and filtered with 0.45 µm syringe membrane filters. The ciprofloxacin concentrations were measured at the maximum wavelength of 270 nm in phosphate buffer using Shimadzu UV-1800 spectrophotometer.

The effects of solution pH (3.0, 5.0, 7.0 and 9.0), catalyst dosage (0.5, 1.0 and 2.0 g/L), H₂O₂ (5, 10 and 20 mM) and water matrix components (2 mM, bicarbonate, sulfate, chloride, nitrate) on the photocatalytic degradation were investigated.

The stability tests were carried out by using the similar procedure as above and the product underwent consecutive cycles. Each cycle lasted for 240 min and the catalyst was centrifuged, washed with deionized water, and added to fresh CIP solution after each cycle.

2.5. Experimental design procedure

In order to optimize the photocatalytic removal of ciprofloxacin, 2³ Box-Behnken design with the total number of 17 experiments including five replicates at the center points was used for response surface modeling. STATISTICA (Ver. 8.0, StatSoft Inc., USA) software package was used for regression and graphical analyses. Three independent parameters, (x₁) catalyst dosage, (x₂) solution pH and (x₃) oxidant (H₂O₂) concentration were varied for the optimization of CIP photodegradation on TiO₂/B 8% (wt.) catalyst. The operating levels of the independent variables are given in Table 1. The predicted response (Y) was selected as the degradation percentage.

3. Results and discussion

3.1. Catalysts characterization

According to the UV-vis diffuse reflectance spectra (Fig.1), the E_g values of catalysts were found decreasing with increasing boron content. The E_g values of raw TiO₂, TiO₂/B 2%, TiO₂/B 4%, TiO₂/B 6% and TiO₂/B 8% were found as 3.09, 3.04, 2.98, 2.91 and 2.88, respectively. The decrease in the band gap values can be ascribed to the presence of oxygen vacancies [19] or to the low mixing of (2p) boron bands with (2p) oxygen bands [20, 22].

Table 1. Levels of independent variables for CIP degradation

Level	Independent variables		
	x ₁ , Catalyst dosage (g.L ⁻¹)	x ₂ , Solution pH	x ₃ , H ₂ O ₂ Concentration (mM)
-1	0.5	5.6	5
0	1.0	7.0	7
1	2.0	9.0	10

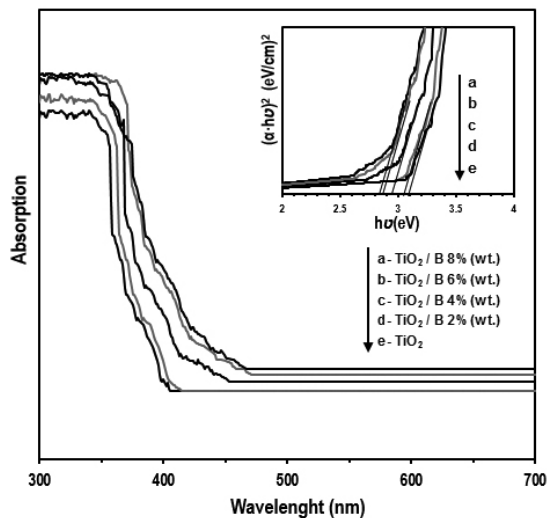


Figure 1. UV-vis diffuse reflectance spectra of the catalysts. Inset shows the Kubelka-Munk transformed reflectance spectra

Figure 2 represents the SEM micrographs obtained for the raw and boron doped TiO_2 catalysts. SEM images of raw TiO_2 sample exhibited smooth crystal structure

and particles are uniform in size while multiple cracks and roughly spherical-shaped grains exist on the surface after boron doping.

3.2. Photocatalytic activity measurements

3.2.1. Effect of boron doping under UV-A and visible light irradiation

In order to compare the CIP photocatalytic degradation efficiencies of TiO_2 and TiO_2/B catalysts, the experiments were carried out under UV-A and visible light illumination and the results are shown in Figure 3. A blank test using CIP solution without catalyst under UV-A irradiation was conducted and no self-degradation of CIP was obtained. About 120 min after initiation, 93.3% of the CIP was decomposed by raw TiO_2 while 97.5% of the CIP was degraded by TiO_2/B 8% catalyst. Under visible light irradiation, degradation of ciprofloxacin effectively increased when boron doped TiO_2 was used as catalyst. In the presence of TiO_2/B 8% (wt.) catalyst, 88.32% of CIP was degraded within irradiation of 240 min. In the control experiments with TiO_2 catalyst, little degradation (19.27%) of CIP was observed after 240 min under visible light irradiation.

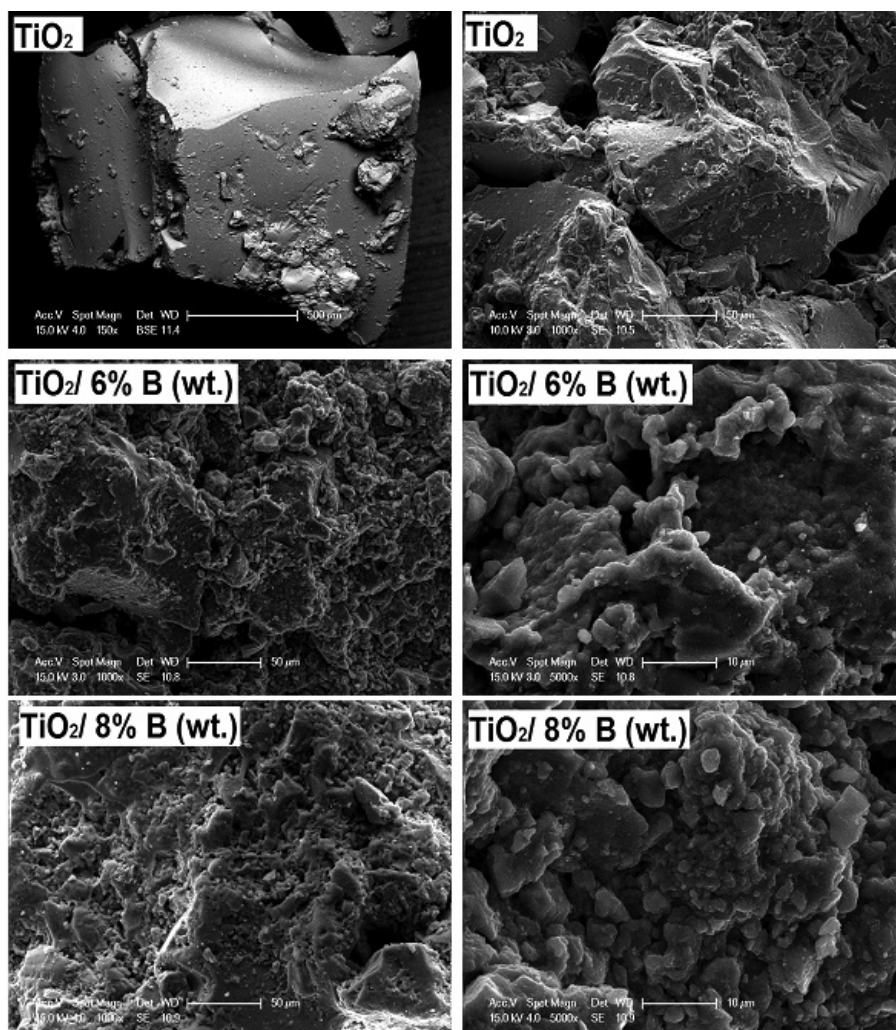


Figure 2. SEM micrographs of raw and boron doped TiO_2 catalysts

ation. With increasing ratio of boron from 2% to 8%, the photocatalysts exhibit greatly enhanced catalytic performance toward ciprofloxacin. TiO₂/B 2% (wt.) catalyst showed slightly higher photo-activity when compared with raw TiO₂. The photocatalytic performances under visible light illumination were found in the order of TiO₂/B 8% > TiO₂/B 6% > TiO₂/B 4% > TiO₂/B 2% > TiO₂ indicating that the decrease in the forbidden band gap plays a significant role in the behavior of catalysts. On the other hand, other factors such as new chemical bonds B–O–Ti and B–O–B in interstitial positions [18] can influence the photo-activity of the catalysts.

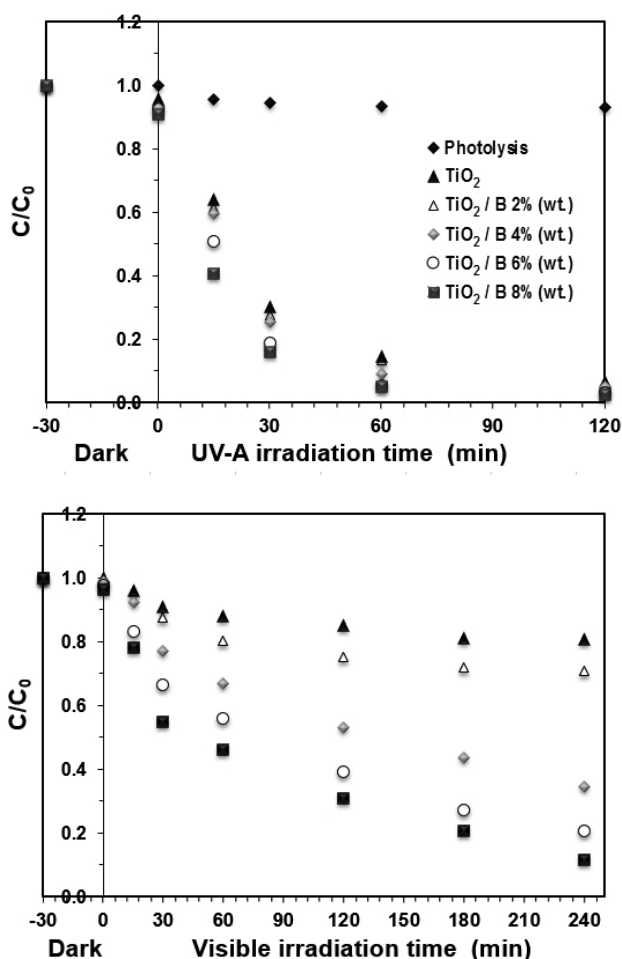


Figure 3. Comparison of the photocatalytic activities of TiO₂ and B-TiO₂ catalysts under UV-A and visible light irradiation [pH=5.6, T= 25–30°C, C₀= 20 mg.L⁻¹, Catalyst dosage=1 g.L⁻¹]

Under visible light, the ciprofloxacin degradation mechanism is proposed via the charge-transfer process at the aqueous-TiO₂ interface [30]. As illustrated in Figure 4, a coordination complex of ciprofloxacin–TiO₂ can be activated by visible light (i), the photo-excited electrons (ii) of CIP triplet migrate to the conduction band of TiO₂ (iii), and the electron in the conduction band recombines with donor molecule or is transferred to an adsorbed conduction band electron acceptor (iv).

The degradation kinetics was fitted using *Langmuir–Hinshwood* kinetic model:

$$\ln\left(\frac{C}{C_0}\right) = -k_{app} t \quad (1)$$

where k_{app} (min⁻¹) is the apparent constant of pseudo-first-order and C_0 and C are the concentrations of CIP at irradiation time of 0 and t . The calculated rate constants (k_{app}) under were listed in Table 2. The photo-activity was found highly dependent on both light source and boron amount. Under UV-A light irradiation, the rate constant of TiO₂/B 6% catalyst was found as $1.615 \times 10^{-2} \text{ min}^{-1}$ while it decreased to $0.600 \times 10^{-2} \text{ min}^{-1}$ under visible light. As the photon energy is lower in visible light [31], the degree of light absorption by the catalyst surface was significantly reduced and lower kinetic constant values were obtained.

On the other hand, k_{app} values increased with increasing boron content both in UV-A and visible light irradiation. Under visible light illumination, the reaction rate constants of the system with TiO₂/B 6% ($k_{app} = 0.600 \times 10^{-2} \text{ min}^{-1}$) and TiO₂/B 8% catalysts ($k_{app} = 0.774 \times 10^{-2} \text{ min}^{-1}$) were about 10 times greater than that of raw TiO₂ ($k_{app} = 0.071 \times 10^{-2} \text{ min}^{-1}$).

3.2.2. Effect of catalyst dosage

As the excess dosages of the catalyst can effect in unfavorable light scattering and decrease the photon absorption efficiency, the catalyst dosage should be optimized for maximum degradation [32]. The effect of catalyst (TiO₂/B 8%) dosage on the degradation of CIP was studied with the dosages varied from 0.5 g L⁻¹ to 2.0 g L⁻¹. As seen in Figure 5(a), when the catalyst dosage increased from 0.5 g L⁻¹ to 1.0 g L⁻¹, k_{app} values increased from 0.202×10^{-2} to $0.774 \times 10^{-2} \text{ min}^{-1}$. Increments in the degradation efficiency within k values can be attributed with the increment in the active sites available for CIP degradation. Further increase has a slight effect on the photocatalytic performance and k values increased slightly to $0.976 \times 10^{-2} \text{ min}^{-1}$ which could be associated with the difficult light penetration and the decrease in number of active sites by catalyst agglomeration [32, 33]. Therefore, 1.0 g L⁻¹ catalyst dosage was chosen adequate for further experiments.

3.2.3. Effect of initial solution pH

As fluoroquinolones are amphoteric substrates, photocatalytic performance is expected to be pH-dependent [34]. Thus, the degradation of CIP at acidic (pH 3.0), basic (pH 9.0) and neutral (pH 7.0) conditions were examined and compared with natural solution pH of 5.6 (Fig. 5(b)). The degradation rate of CIP was found to be highly pH-dependent. The degradation as rather slow at pH 3 and the removal increased from 39.3% (at pH 3.0) to 88.3% (at pH 5.6) while it decreased to 60.0% at pH 9.0. The order of CIP degradation follows pH 3.0 < pH 9.0 < pH 7.0 ≤ pH_{Natural} 5.6.

As the acid dissociation constants of CIP are 6.1 (pK_{a1}) and 8.7 (pK_{a2}), the cationic form of ciprofloxacin

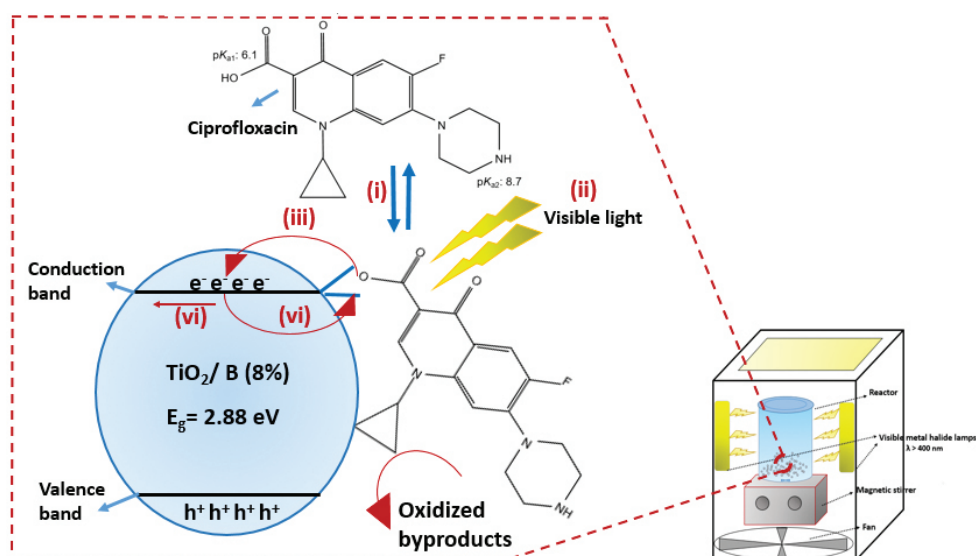


Figure 4. Proposed mechanism for visible-light-activated photocatalytic degradation of ciprofloxacin

Table 2. The rate constants k_{app} and R^2 values of photocatalysts

	UV-A light illumination		Visible light illumination	
	$k_{app} \times 10^{-2} \text{ (min}^{-1}\text{)}$	R^2	$k_{app} \times 10^{-2} \text{ (min}^{-1}\text{)}$	R^2
TiO ₂	1.366	0.989	0.071	0.861
TiO ₂ /B (2%)	1.448	0.989	0.122	0.844
TiO ₂ /B (4%)	1.441	0.981	0.408	0.978
TiO ₂ /B (6%)	1.615	0.939	0.600	0.983
TiO ₂ /B (8%)	1.645	0.945	0.774	0.979

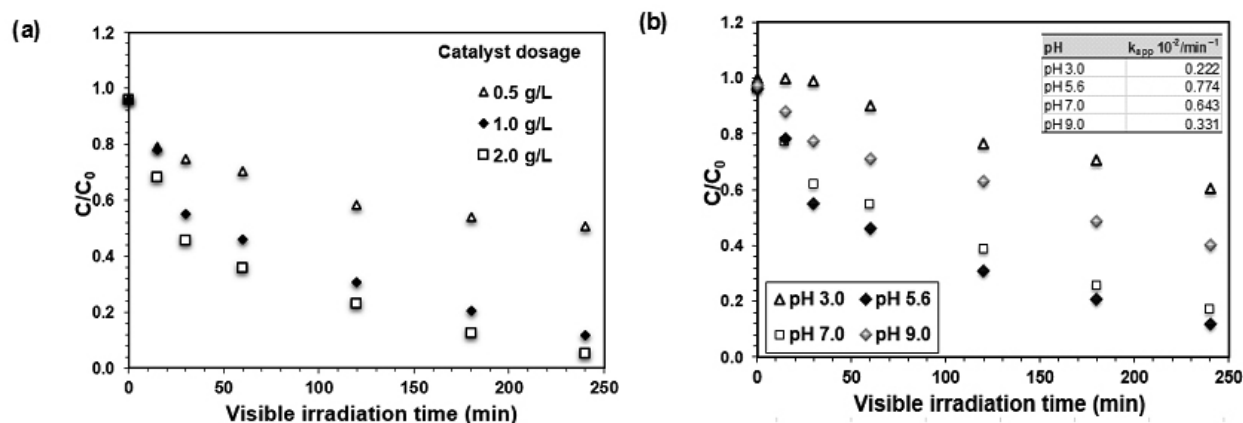


Figure 5. Effect of (a) catalyst dosage and (b) pH on CIP photodegradation

prevailed at $\text{pH} < 6.1$ owing to the protonation of the amine group in the piperazine moiety [6] and thus degradation efficiency was low. At the increased pH (5.6–7.0), the degradation rate was much faster than that at pH 3. In this pH region, CIP keeps almost electroneutral [4], and CIP molecule has a moderate interaction with the catalyst surface. When the solution pH increased from 3.0 to 5.6, the rate constants increased from 0.222 to $0.774 \times 10^{-2} \text{ min}^{-1}$. At pH 9.0, due

to the loss of a proton from the carboxylic group, CIP molecules exist as anions (CIP^-) and the degradation decreased associated with the electrostatic repulsion forces between CIP and the catalyst.

3.2.4. H_2O_2 effect

As the hydrogen peroxide (H_2O_2) in the solution can function as an electron acceptor generating reactive oxygen species, titanium peroxide complex is formed

resulting higher visible-light photoactivity. As seen in Figure 6(a), the synergy degradation activity of the catalyst and H_2O_2 is higher than that of single catalyst system. With an increase in the H_2O_2 concentration from 0 to 10 mM, within 180 min, the degradation increased from 79.4% to 93.2%, respectively. Possible mechanism can be explained as H_2O_2 could react with $\bullet O_2^-$ forming hydroxyl radical ($\bullet OH$) and reduce the possibility for the electron-hole pair recombination [35]. Thus, an electron-hole pair is formed with a suitable energy and the holes are involved in the hydroxyl radicals enabling superior degradation.

3.2.5. Effect of co-existing water matrix chemicals

In order to examine the inhibitory effects on photocatalytic activity, the effect of Cl^- , HCO_3^- , NO_3^- and SO_4^{2-} ions (C_i : 2 mM) as co-existing water matrix components has been studied. As shown in Fig. 6(b), the presence of anions inhibited the CIP degradation and the order of significance was found as $HCO_3^- > SO_4^{2-} > NO_3^- > Cl^-$. This could be related with the fact that the anions can scavenge h^+ or/and $OH\bullet$ forming ionic radicals which are less reactive than h^+ and $OH\bullet$ [36].

3.2.6. Optimization of the photocatalytic removal process

Table 3 presents the ANOVA results of the response surface model of CIP degradation by TiO_2/B 8% catalyst. The results indicated that interactions of catalyst dosage, solution pH and oxidant (H_2O_2) concentration were highly significant since p values were less than the chosen significance level of 0.05. However, the quadratic effect of H_2O_2 concentration was found insignificant and ignored due to the higher p value ($p = 0.4397$). The values of R^2 and R^2_{Adj} were obtained as 0.9960 and 0.9921 respectively, suggesting that the estimated regression equation can be used to predict the degradation efficiency of CIP antibiotic within the experimental range.

By neglecting the insignificant term (x_3^2), the second order polynomial model for CIP degradation -in the chosen range- was described as:

$$Y(\text{Degradation efficiency, \%}) = -72.0503 + 142.04x_1 + 21.349x_2 + 0.293x_3 - 1.516x_1x_2 - 1.030x_1x_3 + 0.374x_2x_3 - 40.959x_1^2 - 1.739x_2^2 \quad (2)$$

Table 3. ANOVA of CIP degradation

	Sum of Squares	df	Mean Square	F value	p value
x_1	1891.837	1	1891.837	1012.708	0.000000
x_1^2	1663.278	1	1663.278	890.360	0.000000
x_2	212.135	1	212.135	113.557	0.000014
x_2^2	97.042	1	97.042	51.947	0.000176
x_3	145.089	1	145.089	77.666	0.000049
x_3^2	1.253	1	1.253	0.671	0.439721
$x_1 \cdot x_2$	16.261	1	16.261	8.704	0.021397
$x_1 \cdot x_3$	16.058	1	16.058	8.596	0.021966
$x_2 \cdot x_3$	10.463	1	10.463	5.601	0.049854
Error	13.077	7	1.868		
Total SS	3632.759	16			
$R^2 = 0.9964$; $R^2_{Adj} = 0.9917$					
After neglecting the insignificant term (x_3^2)					
x_1	1892.200	1	1892.200	1056.355	0.000000
x_1^2	1672.178	1	1672.178	933.524	0.000000
x_2	211.933	1	211.933	118.315	0.000005
x_2^2	98.445	1	98.445	54.959	0.000075
x_3	144.144	1	144.144	80.471	0.000019
$x_1 \cdot x_2$	16.015	1	16.015	8.940	0.017333
$x_1 \cdot x_3$	16.053	1	16.053	8.962	0.017238
$x_2 \cdot x_3$	10.470	1	10.470	5.845	0.042006
Error	14.330	8	1.791		
Total SS	3632.759	16			
$R^2 = 0.99606$; $R^2_{Adj} = 0.99211$					

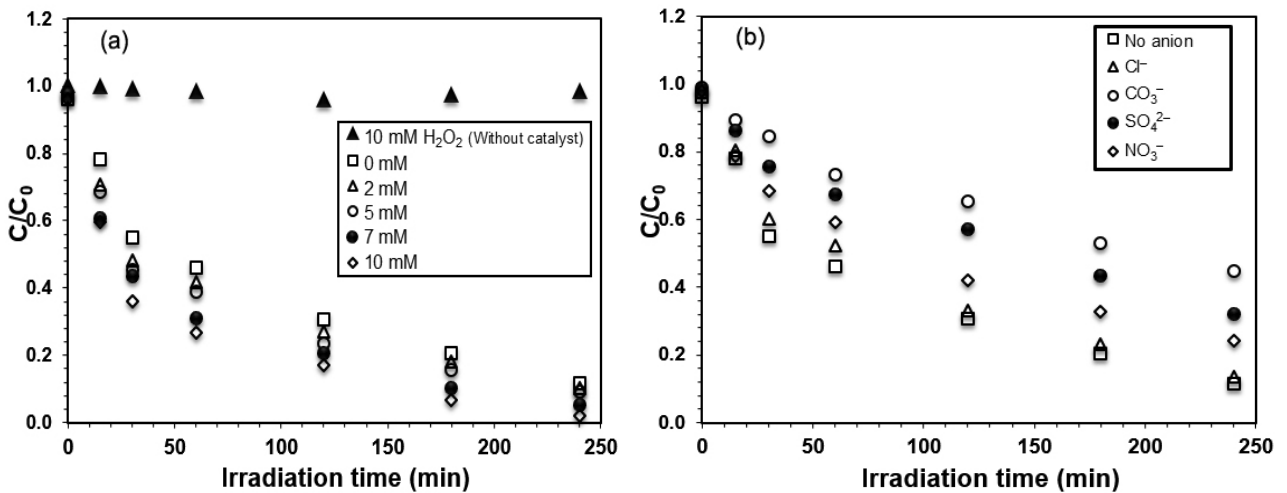


Figure 6. Effect of (a) H_2O_2 and (b) anion on photocatalytic degradation of CIP

The Pareto chart (Fig. 7) shows the effects of the independent variables and their interactions on the degradation efficiency. The magnitude of the t values indicates the significance of corresponding parameter in the model. The linear (x_1 , $t = 32.501$) and quadratic (x_1^2 , $t = 30.553$) terms of catalyst dosage were found to be the most effective variance where linear term of solution pH (x_2 , $t = -10.877$) showed unfavorable effect on the degradation efficiency. The interaction of $x_1 \cdot x_3$ ($t = -2.993$) and $x_1 \cdot x_2$ ($t = -2.990$) also imposed an unfavorable or antagonistic effect on the degradation.

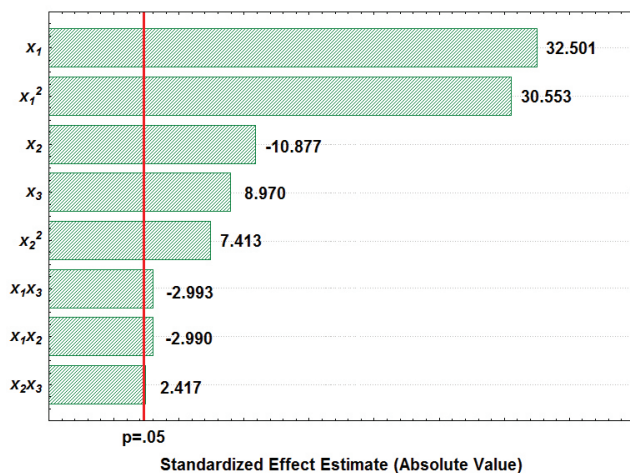


Figure 7. Pareto graphic analysis for the degradation efficiency of CIP by $TiO_2/8\% B$ (wt.) catalyst

Figure 8 shows the three-dimensional response surface plots to illustrate the interaction effects of selected factors on the degradation efficiency of CIP. Fig.8 (a) show the simultaneous influence of H_2O_2 concentration and pH on degradation. At a constant catalyst dose (1 g/L), the degree of degradation increased with increasing pH up to ~ 7 and then decreased. When the solution pH decreased from 9.0 to 7.0 and H_2O_2 concentration decreased from 10.0 to 7.0 mM, the antibiotic degradation increased from 94.5% to 96.6% indicating solution pH was much more significant variable

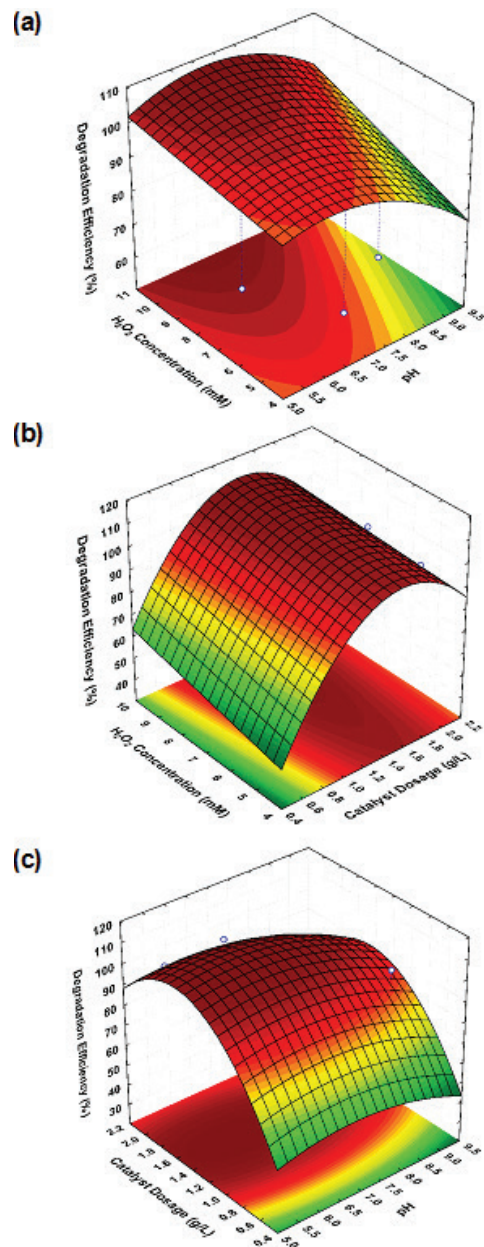


Figure 8. Three-dimensional response surface plots of degradation efficiency of CIP by $TiO_2/8\% B$ (wt.) catalyst

on the photocatalytic removal. The effect of catalyst dose and solution pH is shown in Figure 8 (b). At constant oxidant concentration of 7 mM and pH of 9.0, the degradation percentage increased from 54.6% (dose = 0.5 g/L) to 82.4% (dose = 2.0 g/L). As the amount of $\text{TiO}_2/8\% \text{ B}$ (wt.) catalyst was increased, degradation percent was increased and reached the maximum at about 1.2–1.4 g/L. The slight decrease in degradation from a certain dose of photocatalyst could be related with the increased opacity of the suspension [37]. Consequently, it is indicated from the surface plots that the highest antibiotic degradation was achieved at middle values of three independent factors.

To determine the optimum amount of variables for the highest degradation efficiency of ciprofloxacin, the desirable goal in degradation was set on the maximum value in the chosen range. The maximum percentage degradation was predicted under optimum conditions of catalyst dose of 1.1 g/L, pH 7.14 and H_2O_2 concentration of 7.23 mM.

3.2.7. Catalyst stability

The stability of B- TiO_2 photocatalyst was evaluated via the cycled experiments under visible light irradiation. Moreover, in order to examine the boron leaching effect in the degradation tests, boron concentrations were analyzed in the aliquots at time intervals for each cycle. It was found that no boron was leached after five consecutive runs. As shown in Figure 9, the degradation curves are very close to each other after being

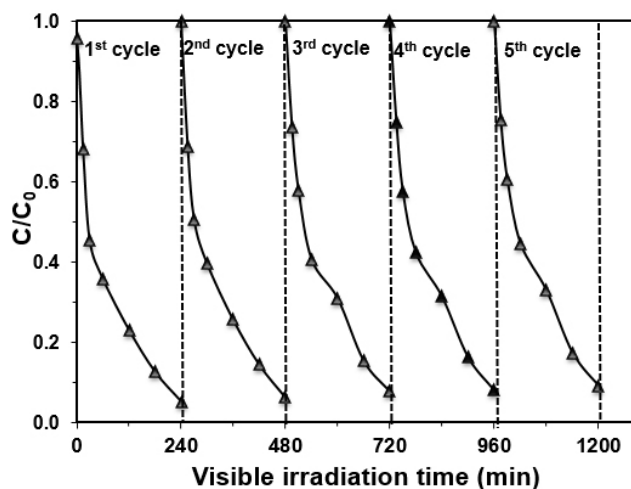


Figure 9. Reusability of $\text{TiO}_2/8\% \text{ B}$ (wt.) catalyst within five consecutive experimental runs [$C_0 = 20 \text{ mg}\cdot\text{L}^{-1}$, Catalyst dosage = $2 \text{ g}\cdot\text{L}^{-1}$, $\text{pH}_{\text{natural}} = 5.6$]

used repetitively for five times and 90.9% of degradation was observed at fifth cycle reflecting that $\text{TiO}_2\text{-B}$ catalyst is very effective and stable under visible light irradiation.

4. Concluding remarks

In the current work, visible light activated boron-doped TiO_2 catalysts have been synthesized by solvothermal method. Compared with raw TiO_2 , B-doped catalysts possessed high photocatalytic performance for the degradation ciprofloxacin antibiotic associated with the decreased band gap energy. Addition of hydrogen peroxide enhanced the degradation efficiency while the radical scavengers reduced the removal slightly indicating that the main controlling mechanism was associated with the free radicals. Based on the statistical modelling results, the optimal conditions for the maximum degradation of ciprofloxacin were as follows: catalyst dosage = 1.1 g/L, solution pH = 7.1 and H_2O_2 concentration = 7.23 mM. Moreover, catalyst dosage and pH were found as the most significant factors effecting the degradation efficiency. After being used repetitively for 5 times and 90.9% of degradation was observed at fifth cycle representing high stability of the catalyst.

Acknowledgments

This study was supported by Yalova University (project no. 2015/BAP/100).

References

- [1] Lu Y., Jiang M., Wang C., Wang Y., Yang W., Impact of molecular size on two antibiotics adsorption by porous resins, *J. Taiwan Inst. Chem. E.*, 45, 955–961, 2014.
- [2] Hassani A., Khataee A., Karaca S., Photocatalytic degradation of ciprofloxacin by synthesized TiO_2 nanoparticles on montmorillonite: Effect of operation parameters and artificial neural network modeling, *J. Mol. Catal. A: Chem.*, 409, 149–161, 2015.
- [3] Jalali H. M., Carlo M., Kinetic study of antibiotic ciprofloxacin ozonation by MWCNT/ MnO_2 using Monte Carlo simulation, *Mater. Sci. Eng. C*, 59, 924–929, 2016.
- [4] Zhang X., Li R., Jia M., Wang S., Huang Y., Chen C., Degradation of ciprofloxacin in aqueous bismuth oxybromide (BiOBr) suspensions under visible light irradiation: A direct hole oxidation pathway, *Chem. Eng. J.*, 274, 290–297, 2015.
- [5] Tu J., Yang Z., Hu C., Qu J., Characterization and reactivity of biogenic manganese oxides for ciprofloxacin oxidation, *J. Env. Sci.*, 26, 1154–1161, 2014.
- [6] El-Shafey E. I., Al-Lawati H., Al-Sumri A. S., Ciprofloxacin adsorption from aqueous solution onto chemically prepared carbon from date palm leaflets, *J. Env. Sci.*, 24, 1579–1586, 2012.
- [7] Batchu S. R., Panditi V. R., ÓShea K. E., Gardinali P. R., Photodegradation of antibiotics under simulated solar radiation: Implications for their environmental fate, *Sci. Tot. Env.*, 470-471, 299–310, 2014.
- [8] Wang H., Li J., Huo P., Yan Y., Guan Q., Preparation of $\text{Ag}_2\text{O}/\text{Ag}_2\text{CO}_3/\text{MWNTs}$ composite photocatalysts for enhancement of ciprofloxacin degradation, *Appl. Surf. Sci.*, 366, 1–8, 2016.

- [9] Wang H., Li J., Ma C., Guan Q., Lu Z., Huo P., Yan Y., Melamine modified P25 with heating method and enhanced the photocatalytic activity on degradation of ciprofloxacin, *Appl. Surf. Sci.*, 329, 17–22, 2015.
- [10] Haddad T., Kümmerer K., Characterization of photo-transformation products of the antibiotic drug Ciprofloxacin with liquid chromatography–tandem mass spectrometry in combination with accurate mass determination using an LTQ-Orbitrap, *Chemosphere*, 115, 40–46, 2014.
- [11] Shi W., Yan Y., Yan X., Microwave-assisted synthesis of nano-scale BiVO₄ photocatalysts and their excellent visible-light-driven photocatalytic activity for the degradation of ciprofloxacin, *Chem. Eng. J.*, 215–216, 740–746, 2013.
- [12] Sturini M., Speltini A., Maraschi F., Pretali L., Profumo A., Fasani E., Albini A. et al., Photodegradation of fluoroquinolones in surface water and antimicrobial activity of the photoproducts, *Water Res.*, 46, 5575–5582, 2012.
- [13] Li C., Chen G., Sun J., Rao J., Han Z., Hu Y., Doping effect of phosphate in Bi₂WO₆ and universal improved photocatalytic activity for removing various pollutants in water, *Appl. Catal. B*, 188, 39–47, 2016.
- [14] Chang C., Fu Y., Hu M., Wang C., Shan G., Zhu L., Photodegradation of bisphenol A by highly stable palladium-doped mesoporous graphite carbon nitride (Pd/mpg-C₃N₄) under simulated solar light irradiation, *Appl. Catal. B*, 143, 553–560, 2013.
- [15] Wang Q., Jiang H., Zang S., Li J., Wang Q., Gd, C, N and P quaternary doped anatase-TiO₂ nano-photocatalyst for enhanced photocatalytic degradation of 4-chlorophenol under simulated sunlight irradiation, *J. Alloys Compd.*, 586, 411–419, 2014.
- [16] Hong Y., Ren A., Jiang Y., He J., Xiao L., Shi W., Sol-gel synthesis of visible-light-driven Ni_(1-x)Cu_(x)Fe₂O₄ photocatalysts for degradation of tetracycline, *Ceram. Int.*, 41, 1477–1486, 2015.
- [17] Xu D., Liu K., Shi W., Chen M., Luo B., Xiao L., Gu W., Ag-decorated K₂Ta₂O₆ nanocomposite photocatalysts with enhanced visible-light-driven degradation activities of tetracycline (TC), *Ceram. Int.*, 41, 4444–4451, 2015.
- [18] Liang L., Yulin Y., Xinrong L., Ruiqing F., Yan S., Shuo L., Direct synthesis of B-doped TiO₂ and its photocatalytic performance on degradation of RhB, *Appl. Surf. Sci.*, A, 265, 36–40, 2013.
- [19] Wu Y., Xing M., Zhang J., Gel-hydrothermal synthesis of carbon and boron co-doped TiO₂ and evaluating its photocatalytic activity, *J. Hazard. Mater.*, 192, 368–373, 2011.
- [20] Quiñones D. H., Rey A., Álvarez P. M., Beltrán F. J., Li Puma G., Boron doped TiO₂ catalysts for photocatalytic ozonation of aqueous mixtures of common pesticides: Diuron, o-phenylphenol, MCPA and terbuthylazine, *Appl. Catal. B*, 178, 74–81, 2015.
- [21] Lan X., Wang L., Zhang B., Tian B., Zhang J., Preparation of lanthanum and boron co-doped TiO₂ by modified sol-gel method and study their photocatalytic activity, *Catal. Today*, 224, 163–170, 2014.
- [22] Zaleska A., Grabowska E., Sobczak J. W., Gazda M., Hupka J., Photocatalytic activity of boron-modified TiO₂ under visible light: The effect of boron content, calcination temperature and TiO₂ matrix, *Appl. Catal. B*, 89, 469–475, 2009.
- [23] Zheng J., Liu Z., Liu X., Yan X., Li D., Chu W., Facile hydrothermal synthesis and characteristics of B-doped TiO₂ hybrid hollow microspheres with higher photocatalytic activity, *J. Alloys Compd.*, 509, 3771–3776, 2011.
- [24] Cavalcante R. P., Dantas R. F., Bayarri B., González O., Giménez J., Esplugas S., Junior A. M., Synthesis and characterization of B-doped TiO₂ and their performance for the degradation of metoprolol, *Catal. Today*, 252, 27–34, 2015.
- [25] Khan R., Woo S., Kim T., Nam C., Comparative study of the photocatalytic performance of boron – iron Co-doped and boron-doped TiO₂ nanoparticles, *Mater. Chem. Phys.*, 112 (1), 167–172, 2008.
- [26] Zhao W., Ma W., Chen C., Zhao J., Shuai Z., Efficient degradation of toxic organic pollutants with Ni₂O₃/TiO_{2-x}B_x under visible irradiation, *J. Am. Chem. Soc.*, 126 (15), 4782–4783, 2004.
- [27] Štengl V., Houšková V., Bakardjieva S., Murafa N., Photocatalytic activity of boron-modified titania under UV and visible-light illumination, *Appl. Mater. Inter.*, 2 (2), 575–580, 2010.
- [28] Uddin N., Islam S., Mazumder M. R., Hossain A., Elias M., Siddiquey I. A., Susan A. B. H., et al., Photocatalytic and antibacterial activity of B/N/Ag co-doped CNT–TiO₂ composite films, *J. Incl. Phenom. Macrocycl. Chem.*, 82, 229–234, 2015.
- [29] Wang B., Leung M. K. H., Lu X. Y., Chen S. Y., Synthesis and photocatalytic activity of boron and fluorine codoped TiO₂ nanosheets with reactive facets, *Appl. Energy*, 112, 1190–1197, 2013.
- [30] Paul T., Miller P., Strathmann T., Visible-Light-Mediated TiO₂ Photocatalysis of Fluoroquinolone Antibacterial Agents, *Environ. Sci. Technol.*, 41, 4720–4727, 2007.
- [31] Dobrosz-Gómez I., Gómez-García M. A., López Zamora S. M., GilPavas E., Bojarska J., Kozanecki M., Rynkowski J. M., Transition metal loaded TiO₂ for phenol photo-degradation, *C. R. Chimie*, 18, 1170–1182, 2015.
- [32] Mao X., Fan C., Wang Y., Wang Y., Zhang X., RhB-sensitized effect on the enhancement of photocatalytic activity of BiOCl toward bisphenol-A under visible light irradiation, *Appl. Surf. Sci.*, 317, 517–525, 2014.
- [33] Vaiano V., Iervolino G., Sannino D., Rizzo L., Sarno G., Farina A., Enhanced photocatalytic oxidation of arsenite to arsenate in water solutions by a new catalyst based on MoO_x supported on TiO₂, *Appl. Catal. B*, 160–161, 247–253, 2014.
- [34] Razuc M., Garrido M., Caro Y. S., Teglia C. M., Goicoechea H. C., Fernández B. S., Hybrid hard- and soft-modeling of spectrophotometric data for monitoring of ciprofloxacin and its main photodegradation products

- at different pH values, *Spectrochim. Acta Part A*, 106, 146–154, 2013.
- [35] Rong X., Qiu F., Rong J., Zhu X., Yan J., Yang D., Enhanced visible light photocatalytic activity of W-doped porous, *Mater. Lett.*, 164, 127–131, 2016.
- [36] Hou D., Goei R., Wang X., Wang P., Lim T., Preparation of carbon-sensitized and Fe–Er codoped TiO₂ with response surface methodology for bisphenol A photocatalytic degradation under visible-light irradiation, *Appl. Catal. B*, 126, 121–133, 2012.
- [37] Salarian A. A., Hami Z., Mirzaei N., Mohseni S. M., Asadi A., Bahrami H., Vosoughi M., et al., N-doped TiO₂ nanosheets for photocatalytic degradation and mineralization of diazinon under simulated solar irradiation: Optimization and modeling using a response surface methodology, *J. Mol. Liq.*, 220, 183–191, 2016.